IMPROVEMENT OF FREQUENCY RESPONSE OF WAVEGUIDE-DIAPHRAGM-TYPE RESISTIVE SENSORS FOR HIGH POWER MICROWAVE PULSE MEASUREMENT

(Final report)

Grant-04-3047

Microwave laboratory, Semiconductor Physics Institute
A. Goštauto 11, Vilnius LT 01108, Lithuania
tel.: 370 5 261 9808
fax.: 370 5 262 7123
e-mail: kancleris@uj.pfi.lt

Vilnius, 2005

REPORT DOCUMENTATION PAGE

27Form Approved OMB No. 0704-0188

1. REPORT DATE *(DD-MM-YYYY)*	2. REPORT TYPE	3. DATES COVERED *(From – To)*
07-11-2005	Final Report	1 October 2004 - 01-Oct-05

4. TITLE AND SUBTITLE

Improvement of the Frequency Response of Waveguide-type Resistive Sensors for High-Power Microwave Pulse Measurement

5a. CONTRACT NUMBER
FA8655-04-1-3047

5b. GRANT NUMBER

5c. PROGRAM ELEMENT NUMBER

6. AUTHOR(S)

Dr. Zilvinas Kancleris

5d. PROJECT NUMBER

5d. TASK NUMBER

5e. WORK UNIT NUMBER

7. PERFORMING ORGANIZATION NAME(S) AND ADDRESS(ES)

Semiconductor Physics Institute
Microwave Laboratory
A. Gostauto 11
Vilnius LT-01108
Lithuania

8. PERFORMING ORGANIZATION REPORT NUMBER

N/A

9. SPONSORING/MONITORING AGENCY NAME(S) AND ADDRESS(ES)

EOARD
PSC 802 BOX 14
FPO 09499-0014

10. SPONSOR/MONITOR'S ACRONYM(S)

11. SPONSOR/MONITOR'S REPORT NUMBER(S)
SPC 04-3047

12. DISTRIBUTION/AVAILABILITY STATEMENT

Approved for public release; distribution is unlimited.

13. SUPPLEMENTARY NOTES

14. ABSTRACT

This report results from a contract tasking Semiconductor Physics Institute as follows: The contractor will investigate resistive sensors for measuring high power microwave pulses. At the end of this investigation, the contractor will design, fabricate and test a waveguide-type resistive sensors.

15. SUBJECT TERMS
EOARD, High Power Microwaves, High Power Microwave Sensors

16. SECURITY CLASSIFICATION OF:			17. LIMITATION OF ABSTRACT	18, NUMBER OF PAGES	19a. NAME OF RESPONSIBLE PERSON
a. REPORT	b. ABSTRACT	c. THIS PAGE			MICHAEL KJ MILLIGAN, Lt Col, USAF
UNCLAS	UNCLAS	UNCLAS	UL	27	**19b. TELEPHONE NUMBER** *(Include area code)* +44 (0)20 7514 4955

Contents

1. Introduction....3
2. Waveguide-diaphragm-type resistive sensor....4
   2.1 The sensor....4
   2.2 Sensitivity....5
   2.3 Output signal....6
   2.4 Measurement techniques....10
   2.5 Conclusions....12
3. Factors influencing the average electric field strength in the SE....12
   3.1 Obstacle under the diaphragm....12
   3.2 Optimized sensor....15
   3.3 Conclusions....16
4. Experimental investigation....17
   4.1 Frequency response....17
   4.2 Output signal....21
   4.3 Conclusions....22
5. Extension of dynamic range....23
   5.1 Shift of the sensing element....23
   5.2 Optimization of the characteristic of the RS with shifted SE....26
   5.3 Conclusions....26
6. Conclusions....26
7. References....27
8. Acknowledgement....27

Microwave Laboratory of Semiconductor Physics Institute has performed this work under the contract FA8655-04-1-3407 issued by European Office of Aerospace Research and Development (EOARD). Principal investigator: Žilvinas Kancleris, Dr. Habil., Head of Microwave Laboratory.

1. Introduction

At present, different types of pulsed high power microwave (HPM) oscillators and amplifiers are being researched in laboratories, as well as being manufactured by industry. They are used in communication systems, radars, electromagnetic testing facilities, scientific research, and military projects. Many HPM systems should be continuously monitored for output pulse's power level during manufacturing and operation. The large number of measurements involved and their importance dictate that the measurement equipment and techniques should be accurate, reproducible, and convenient to use.

At a moment, calibrated diodes are mainly used for the measurement of instantaneous or envelope power in a wide frequency range. They are employed for the measurement of HPM pulses as well. Main disadvantage of the diodes when using them for HPM applications is that the diodes can handle only a very low power level. Highest pulse power can be measured by the planar-doped-barrier diodes is of the order of 100-200 mW [1]. Therefore when the diode is used for the measurement of HPM pulses the initial pulse has to be strongly attenuated. From the one hand, large attenuation of the microwave power results in a decrease in measurement accuracy. In addition, the size and weight of the measurement system increases, its control becomes complicated. From the other hand, when measuring pulsed microwave power of the order of mW, the diode outputs a DC pulse with amplitude of the order of mV. To measure such small DC signal in the presence of stray pick-up and electromagnetic interference that are typical to the environment of HPM sources shielded chambers with the measurement equipment situated at a respectful distance from HPM source are usually employed. Installation of shielded chambers confines the flexibility of the measurement system its price increases.

We have developed an alternative device for HPM pulse measurement – resistive sensor (RS) the performance of which is based on electron heating effect in semiconductors. The RS is actually the resistor made from sufficiently high specific resistance n-type Si. It is inserted in the transmission line. The electric field of the microwave pulse traveling in the transmission line heats electrons in the sensing element (SE), its resistance increases, and by measuring this resistance change the microwave pulse power in the transmission line is determined. The main advantages of the RS over the diode are the following: it can measure high power microwave pulses directly, produces high output signal, is overload resistant, and demonstrates very good long term stability. At present both waveguide-type and coaxial-type RS's have been developed. A waveguide-diaphragm-type RS developed in our laboratory consists of the SE that is placed under a thin metal diaphragm that is parallel to wide wall of the waveguide. Such design of the RS is suitable for the measurement of short HPM pulses, the amplitude of which is practically restricted by a breakdown in the waveguide [2]. Waveguide-diaphragm-type RS has been used in Russian, Sweden, Taiwan, Indian and USA microwave centers. Our activities in a waveguide-type RS area have been summarized in a review article [3]. The main drawback of the waveguide-diaphragm-type RS is a large variation of the sensitivity in a waveguide's frequency band. It was shown that the sensitivity of the X-band RS changes in the frequency band more than two times [4]. The same frequency response is likely to be characteristic of the RS in other frequency bands as well. It should bee noted that we have also developed the coaxial-type* RS that can be used over a wide frequency range since this device has a flat frequency response. Unfortunately, it can measure only 1 kW amplitude microwave pulses and this imposes the restriction for HPM application.

---

* The development of the coaxial-type RS was supported by European Office of Aerospace Research and Development under contract number F61775-02-WE030

Having in mind the drawback of the waveguide-diaphragm-type RS, our activities under the current project are concentrated on the elucidation of reasons that result in strong dependence of the average electric field in the SE on frequency. Clarifying regularities of the dependence of the average electric field in the SE on its electrophysical parameters and metal diaphragm length we shall be able to design the waveguide-diaphragm-type RS with flat frequency response within waveguide's frequency band. The goal of this work is to achieve sensitivity variation within waveguide's frequency band less than ±15%.

In the final report theoretical and experimental investigations on the improvement of frequency response of the waveguide-diaphragm-type RS are presented. The report is organized as follows. In Section 2 the principle of the waveguide-diaphragm-type RS design is described, its sensitivity, and experimental investigation techniques are considered. The factors influencing the dependence of the average electric field strength in the SE on frequency are discussed in section 3. Experimental investigation of the waveguide-diaphragm-type RS with the optimized frequency response is presented in Section 4. Section 5 is devoted to the theoretical consideration of the RS measuring HPM pulses at higher power levels.

2. *Waveguide-diaphragm-type resistive sensor*

The structure of the waveguide-diaphragm-type RS is considered in this section. Typical electrophysical parameters of the SE as well as output signal dependences on pulse power and frequency are presented. The reasons that may cause the dependence of the output signal on frequency are considered.

2.1 The sensor

As it was already mentioned in Introduction the performance of the RS is based on electron heating effect in semiconductor. Thus, the SE is actually a resistor made from n- type Si with two Ohmic contacts. Typical arrangement of the SE in the waveguide-diaphragm-type RS devoted for HPM pulse measurement is shown in Figure 1. It is seen that the SE is inserted between thin metal diaphragm and wide wall of the waveguide. Upper contact of the SE is isolated whereas the lower – grounded through the diaphragm. The electric field of microwave pulse traveling in the waveguide heats electrons in the sensor, its resistance increases, and by measuring this resistance change the microwave pulse power in the waveguide is determined. To measure resistance change the SE should be connected to the current source. To increase output signal the source producing DC pulses synchronized with measuring microwave pulse is usually used [3]. It allows getting output signal up to a few tens of Volts without any amplification. It is obvious that the average electric field in the SE depends on electrophysical parameters of the RS. Those parameters can be distinguished in Figure 2 where two layers of the waveguide-diaphragm-type RS are presented. As one can see from the figure, the characteristic dimensions of the RS are the following: a and b are dimensions of the waveguide window, h, d and l are dimensions of the SE, L_d is the length of metal diaphragm, Δx, Δz are the shift of the center of the SE from the

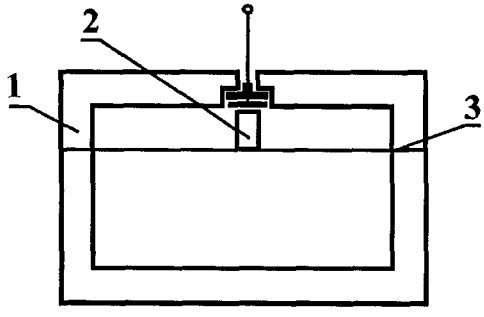

Figure 1. Cross-sectional view of waveguide-diaphragm-type resistive sensor with diaphragm. 1 – waveguide, 2 – sensing element, 3 – metal diaphragm.

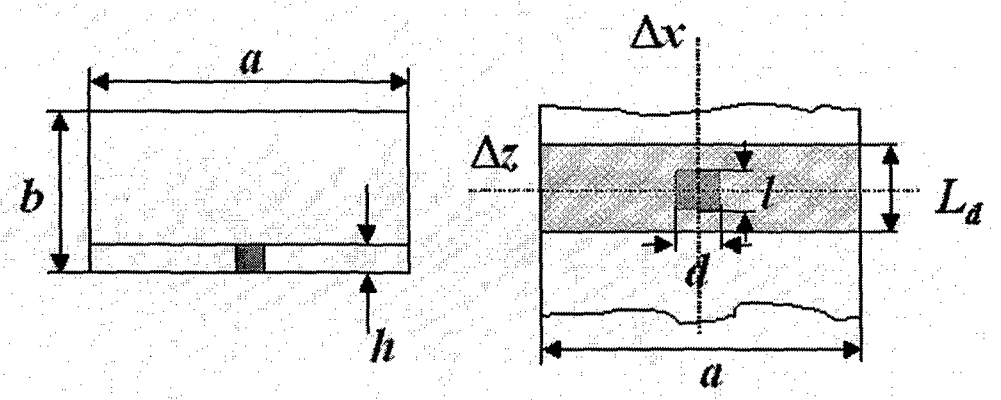

Figure 2. Characteristic dimensions of the waveguide-diaphragm-type RS: a, b – size of waveguide window, h, d, l –height, width and length of the SE, L_d – length of the diaphragm, Δx, Δz possible shift of the SE from the symmetry plane towards narrow wall of the waveguide and in the direction of wave propagation, respectively. In the latter case shift into wave propagation direction is considered as positive, whereas the opposite shift – as negative.

symmetry planes towards narrow wall of the waveguide and in the direction of wave propagation. After adding to them the specific resistance of the n-type Si (ρ, Ω·cm) from which the SE is made one can get a set of nine parameters characterizing the waveguide-diaphragm-type RS. The values of those electrophysical parameters for the typical X band waveguide-diaphragm-type RS are collected in Table 1.

Table 1. Typical electrophysical parameters of the X-band waveguide-diaphragm-type RS.

a, mm	b, mm	h, mm	l, mm	d, mm	L_d, mm	ρ, Ω·cm	Δx, mm	Δz, mm
23	10	1.0	1.75	1.75	9.0	5.0	0.0	0.0

2.2 Sensitivity

Since the RS measures pulse power of microwaves and the resistance change is the quantity indicating power level it is convenient to define a sensitivity of the sensor in linear region in the following way

$$\frac{\Delta R}{R} = \zeta P, \tag{1}$$

where ζ is the sensitivity, $\Delta R/R$ is a relative resistance change of the SE in a microwave electric field, and P is pulse power propagating in the waveguide. Since the relative resistance change is dimensionless quantity, the dimension of sensitivity will be $[\text{power}]^{-1}$. For the RS that is devoted to the measurement of HPM pulses, it is convenient to use kW^{-1}.

Definition (1) is not unique. Sometimes sensitivity is defined as a signal to power ratio. Taking into account that the signal amplitude depends not only on DC voltage drop on the SE but on the input resistance of the measurement unit used for the output signal measurement as well, the proposed definition of the sensitivity is likely more acceptable.

In the linear region, the strength of the electric field in the SE is sufficiently small. This range of electric field is known as warm-electron or slightly heating electric field region. It is well established that the relative resistance change in this region is proportional to the square of the electric field [3]

$$\frac{\Delta R}{R} = \beta^*(f)\langle E_m \rangle^2 \tag{2}$$

where $\beta^*(f)$ is frequency dependent so-called effective warm-electron coefficient in a RF electric field and $\langle E_m \rangle$ is the average amplitude of the RF electric field in the SE. When trying to determine the average electric field strength in the SE it is convenient to use dimensionless ratio $\langle E_m/E_0 \rangle$, normalizing actual electric field amplitude in the SE by the amplitude of the electric field in the center of empty waveguide. The later is described by well-known formulae [5]

$$E_0^2 = \frac{4P\sqrt{\mu_0/\varepsilon_0}}{ab\sqrt{1-(f_c/f)^2}}. \tag{3}$$

Here a and b are dimensions of the waveguide window, μ_0 and ε_0 are vacuum permeability and permittivity, f_c is the cutoff frequency. Making use of (1) to (3) one can get the following expression describing the sensitivity of the waveguide-type RS in a linear region

$$\zeta = \frac{4\beta^*(f)\sqrt{\mu_0/\varepsilon_0}}{ab\sqrt{1-(f_c/f)^2}}\left\langle \frac{E_m}{E_0} \right\rangle^2. \tag{4}$$

Obtained expression is used for the calculation of the RS sensitivity theoretically. To do that the average electric field in the SE has been determined using finite-difference time-domain (FDTD) method. Details of calculations have been presented in our previous report [6]. Except $\langle E_m/E_0 \rangle$, a few multipliers can be found in the expression (4) those influence the dependence of sensitivity of the RS on frequency. Let us consider them in more details.

First, the square root appearing in the denominator of the expression (4) indicates the fact that even at the same power level transmitted through the waveguide the electric field strength in it changes due to wave dispersion (3). In waveguide's frequency band ratio f_c/f changes from 0.8 up to 0.5. Using those values one can easily get that due to wave dispersion the sensitivity of the waveguide-type RS in waveguide frequency range monotonously decreases 1.44 time.

Second, the effective warm electron coefficient is frequency dependent as well. Its dependence on frequency is well described by the following phenomenological expression taking into account the influence of electron heating inertia on resistance change in RF electric field

$$\beta^*(f) = \beta\left[\frac{1}{2} + \frac{1}{1+(2\pi f\tau_\varepsilon)^2}\right], \tag{5}$$

where β is the warm electron coefficient in the DC electric field and τ_ε is a phenomenological energy relaxation time. The value of the latter parameter $\tau_\varepsilon = 2.9\cdot10^{-12}$ s for n-Si at room temperature was determined in [7] by fitting the measured $\beta^*(f)$ in a wide frequency range with (5). Making use of (5) and known value of τ_ε one can estimate the influence of heating inertia on the RS sensitivity. At frequency 12.5 GHz the decrease of β^* is less than 3%. This means that influence of electron heating inertia on the RS performance is negligible up to and including X-band. Nevertheless, at higher frequencies the influence of heating inertia on the RS sensitivity should be taken into account.

2.3 Output signal

For the measurement of the output signal the DC current source should be connected to the RS. To obtain larger output signal and maintaining sensor heating at sufficiently low level DC pulse supply is used for the RS feeding as well [2]. Let us consider both measurement methods in more detail and find the expressions binding experimentally measured quantities with the RS sensitivity in the linear region ζ defined by expression (1).

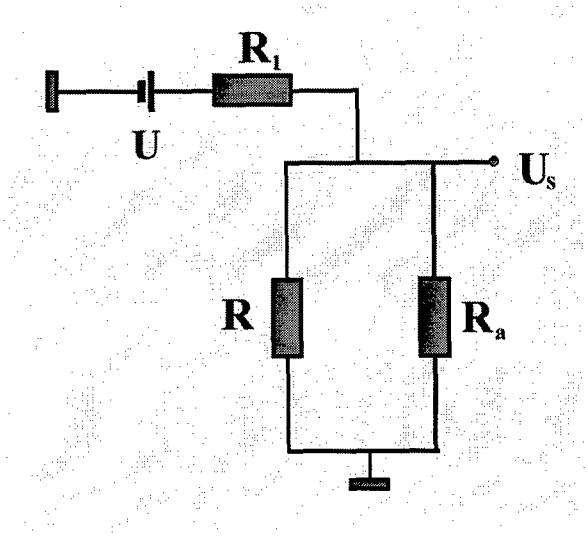

Figure 3. Equivalent circuit for the measuring of the output signal of the RS using current source for sensor feeding: R is a resistance of the RS, R_a is input resistance of the oscilloscope. Constant current source is presented as a DC voltage source followed by resistor R_1, that is much larger than R.

An equivalent circuit for the measurement of the output signal of the RS using constant current sources is presented in Figure 3. As one can see from the figure constant current source in the equivalent circuit is presented by voltage source U followed by resistor R_1. This resistor stands for an internal resistance of the current source. Usually R_1 is chosen much larger than R. Output signal of the RS can be expressed as a difference between voltage U_S that settles when the resistance of the SE increases due to electron heating in a RF electric field and the old value of it in the absence of the microwave pulse:

$$U_S = U_S(R+\Delta R) - U_S(R). \qquad (6)$$

Denoting voltage drop on the SE in the absence of microwave pulse as U_0 one can readily get

$$U_0 = U\frac{RR_a}{RR_a + R_1(R+R_a)}. \qquad (7)$$

The voltage $U_S(R+\Delta R)$ in the presence of microwave pulse can be obtained inserting into (7) $R+\Delta R$ instead of R. Inserting obtained expression and expression (7) into (6) one can finally get

$$U_S = \frac{U_0\dfrac{\Delta R}{R}}{1+\left(\dfrac{R}{R_1}+\dfrac{R}{R_a}\right)\left(1+\dfrac{\Delta R}{R}\right)}. \qquad (8)$$

As it follows from (8) when R_1 and R_a are compatible with the resistance of the SE the output signal of the RS decreases. It is obvious, since as it is seen from equivalent circuit in Figure 3 all resistors are actually connected in parallel. When $R << R_a$, R_1 output signal simply is

$$U_S = U_0\frac{\Delta R}{R}. \qquad (9)$$

It should be noted that the output signal of the RS is usually measured in the nonlinear region as well. As it was shown in [3] the quadratic polynomial fits well the dependence of P on the relative resistance change of the SE inserted in the waveguide in a wide dynamical range, therefore, that dependence can be written down in the following way

$$P = A\frac{\Delta R}{R} + B\left(\frac{\Delta R}{R}\right)^2. \qquad (10)$$

Here values of coefficients A and B are determined by fitting (10) with experimental data in a least square sense. Expression (10) is very useful for the RS calibration. Calibrating the RS the dependence of U_S versus microwave pulse power P is measured and a set of pairs of numbers is determined

$$P_i, U_{Si} \quad i = 1,2,\ldots N. \qquad (11)$$

Making use of (9) measured data are approximated with the polynomial

$$P = A\frac{U_S}{U_0} + B\left(\frac{U_S}{U_0}\right)^2, \tag{12}$$

and in such a way coefficients A and B are determined. Further expression (12) can be used as formulae to determine pulse power in the waveguide from the measured value of the output signal of the RS. Comparing (1) and (10) it is seen that determined from experimental data coefficient A is related with ζ

$$A = 1/\zeta. \tag{13}$$

As it was already mentioned, 50 V DC pulse supply is usually used for the RS feeding [2]. It allows increase measured output signal significantly without using any pulse amplification circuit maintaining average sensor heating at sufficiently low level. This method was successfully applied for the measurement of short HPM pulses [4]. Since in this case more sophisticated scheme is used for sensor feeding and signal measurement, let us consider it in more detail.

The equivalent circuit for the feeding of the RS and the output signal measurement is shown in Figure 4. DC pulse source producing $U_0 = 50$ V DC pulses is used for sensor feeding. The duration of the DC pulse is chosen in such a way that before the microwave pulse is triggered the splitting capacitor C_s is charged up to a voltage U_0. For this reason current flows through the arm of the circuit with the RS only and hence

$$I = I_r = \frac{U_0}{R + R_i}. \tag{14}$$

Since $I_a = 0$, the output signal measured by oscilloscope $U_S = 0$. Microwave electric field induces the resistance change of the SE and the current flowing through it should decrease. Due to the inductance L present in the circuit the current from the DC source I is kept constant during microwave pulse. Therefore, current flowing in the other arm of the circuit should increase by the same amount. Denoting this current change as ΔI and the change of the resistance of the SE as ΔR the voltage drop on the SE can be expressed as

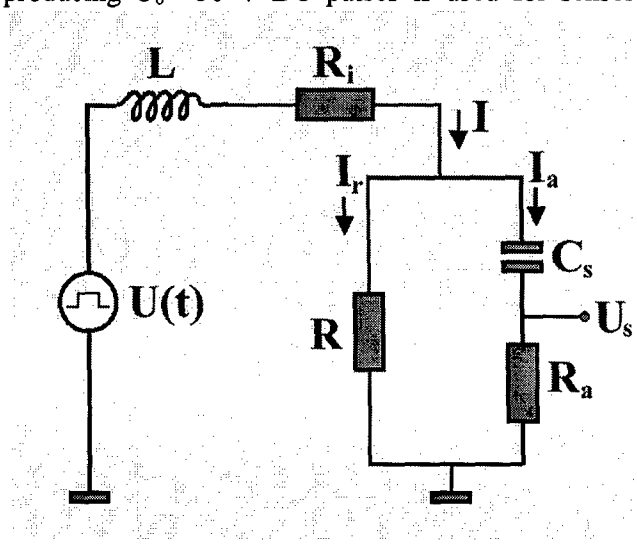

Figure 4. Equivalent circuit for the measuring of the output signal of the RS using DC pulse supply for sensor feeding: $U(t)$ is a source producing DC pulse $U_0 = 50$ V, L is the inductance, R_i denotes an active resistance of the inductance, C_s is a splitting capacitor, R is a resistance of the RS and R_a is an input resistance of the oscilloscope.

$$(I - \Delta I)\cdot(R + \Delta R). \tag{15}$$

This voltage should be equal to the voltage drop on the right arm of the circuit consisting of initial voltage up to which the capacitor was charged before the microwave pulse appears IR and additional voltage drop on the input resistance of the oscilloscope R_a

$$IR + \Delta IR_a. \tag{16}$$

Equating voltage drops on both arms of the circuit (15) and (16) one gets

$$I\Delta R - \Delta IR - \Delta I\Delta R = \Delta IR_a. \tag{17}$$

Measured signal by the oscilloscope is simply $U_S = \Delta I R_a$, therefore inserting into it DI from (17) one easily gets

$$U_S = IR_a \frac{\Delta R}{R_a + R + \Delta R}. \tag{18}$$

As it was already mentioned inductance kept current constant during microwave pulse, thus expression (14) can be used to calculate I. Having in mind that the active resistance of the inductance is always much less than the resistance of the SE $R_i << R$ the output signal measured by the oscilloscope can be expressed as follows

$$U_S = U_0 \frac{\frac{\Delta R}{R}}{1 + \frac{R}{R_a}\left(1 + \frac{\Delta R}{R}\right)}. \tag{19}$$

It should be noted, that this measurement system is devoted to resolve short microwave pulses. Therefore, input impedance of oscilloscope has to be set 50 Ω. Since the resistance of the RS usually is compatible to the input resistance of a measurement device, the ratio R/R_a should be taken into account in expression (19). Denoting it as $\eta = R/R_a$ the relative resistance change can be expressed as a function of the measured signal in the following way

$$\frac{\Delta R}{R} = \frac{(1+\eta)U_S}{U_0 - \eta U_S}. \tag{20}$$

Inserting (20) into (10) the expression being fitted for the experimental data measured using 50 V DC pulse supply can be obtained

$$P = A\frac{(1+\eta)U_S}{U_0 - \eta U_S} + B\left(\frac{(1+\eta)U_S}{U_0 - \eta U_S}\right)^2. \tag{21}$$

As one can see from (21), the value of η influences the output characteristic of the RS. Only

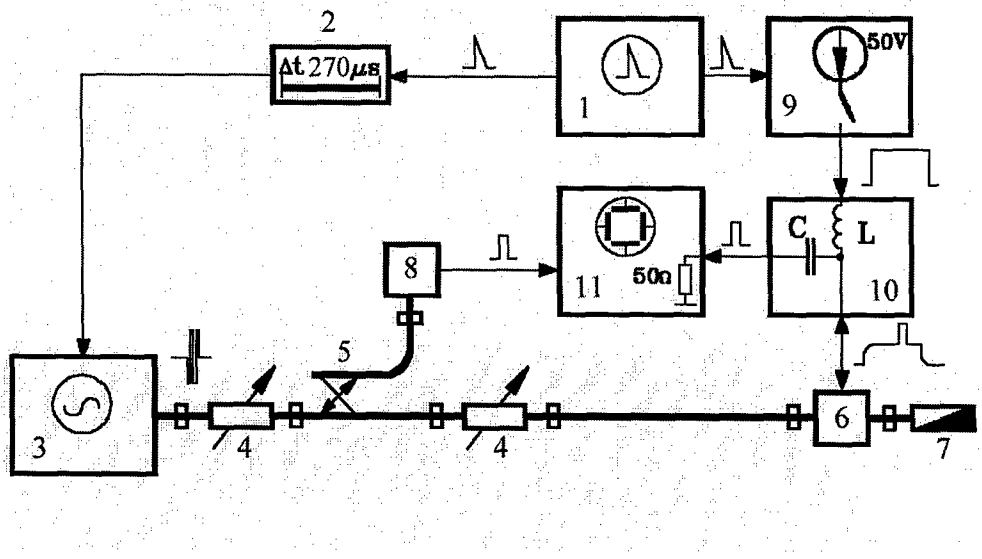

Figure 5. Experimental setup for the measurement of the dependence of output signal of the RS on pulse power: 1 – synchronizing master generator, 2 – delay line, 3 – magnetron, 4 – variable precise attenuators, 5 – directional coupler, 6 – the RS under test, 7 – matched load, 8 – reference pulse power meter, 9 – DC pulse supply, 10 – splitting circuit, 11 – oscilloscope Tektronix TDS 520.

in the case when the resistance of the SE is much less than the input resistance of the oscilloscope output characteristics measured using current source and 50 V DC pulse supply are identical.

2.4 Measurement techniques

For the measurement of the dependence of the output signal of the RS on pulse power the setup presented in Figure 5 was used. A synchronizing master generator 1 switches on a DC pulse generator 9 that produces DC pulses duration and amplitude of which are roughly 300 μs and 50 V, respectively. The repetition frequency of the order of 10 Hz is used in the measurement. The triggering pulse delayed nearly 270-280 μs starts a magnetron generator 3 producing roughly 100 kW pulse power at fixed frequency 9.3 GHz. The duration of the pulse is up to a few microseconds, therefore the feeding pulse covers entire microwave pulse. The coil inductance in the splitting circuit 10 is chosen so that it has a low resistance for the feeding pulse and a high resistance for the measuring one. Therefore, the output signal appears as a short video pulse on the envelope of the feeding pulse. The capacitor in the splitting circuit 10 cuts off the DC pulse and the oscilloscope 11 detects the short video pulse. Using such a scheme for the RS 6 feeding the output signal on the order of a few tens of Volts has been obtained without any amplification.

A reference pulse power meter 8 is connected to the main waveguide via directional coupler 5. The cross-waveguide-type RS is used for this purpose [3]. An oscilloscope measures the signal from it as well. Using first variable attenuator 4 in the main waveguide the same reading of the reference pulse power meter is restored during measurement procedure eliminating in such a way the drift of pulse power generated by the magnetron. The dependence of the output signal of the RS under test on pulse power is measured by gradually increasing losses in the second variable attenuator 4 in the main waveguide.

Frequency response of the RS has been investigated using a TWT pulse generator. It produces roughly 50 W pulses in the frequency range 8-12 GHz. An experimental setup for frequency response measurement is shown in Figure 6. Microwave pulse generated by TWT 1 passes second harmonic filter 2, ferrite insulator 3 and using waveguide switch 4 can be directed either to reference pulse power meter 5 or to the RS under test 6. The RS is followed by matched load 7 and is fed by 50 V DC pulses 9. The dual-channel oscilloscope 8 Tektronix TDS 520 measures signals from the RS and the reference pulse power meter. Reference pulse power meter monitors pulse power level in the waveguide. Since pulse power generated by TWT is sufficiently low, the output signal in the linear region is measured. Thus,

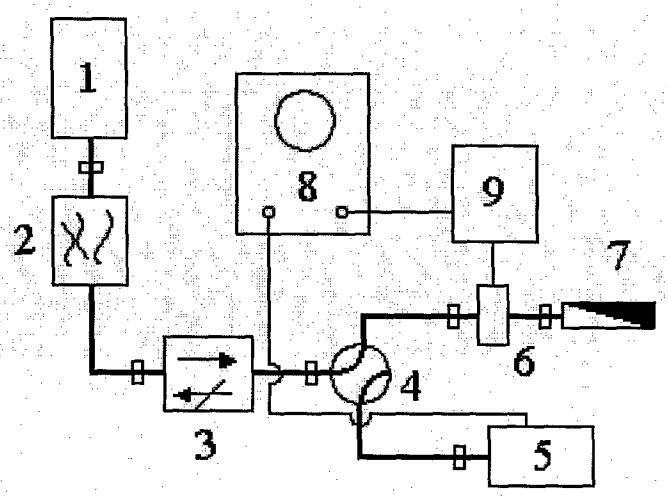

Figure 6. Experimental setup for frequency response measurement: 1 – tunable frequency pulse power source (TWT), 2 – second harmonic filter, 3 – ferrite isolator, 4 – waveguide switch, 5 – reference pulse power meter, 6 – the RS under test, 7 – matched load, 8 – oscilloscope Tektronix TDS 520, 9 – DC pulse supply circuit with signal splitter.

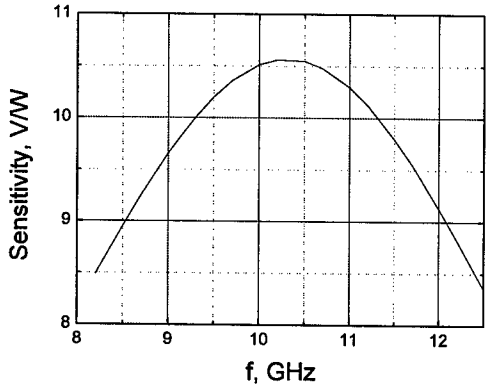

Figure 7. Dependence of the sensitivity on frequency of the cross-waveguide-type RS that is used in the measurements as the reference pulse power meter.

only the first term should be accounted in the expression (21) and to determine the sensitivity of the RS in the linear region ζ the following expression is employed

$$\zeta = \frac{(1+\eta)U_S}{(U_0 - \eta U_S)P}. \qquad (22)$$

As a reference pulse power meter the cross-waveguide-type RS is used [3]. Before performing measurements of the frequency response the reading of the reference pulse power meter is linked with the absolute power level. To do that the power sensor NRV-Z54 of the Rohde & Schwarz reference average power meter NRVS is connected to the arm of the waveguide instead of the RS under test. An average power meter is connected to the waveguide making use of the coaxial to waveguide adapter. Measuring the readings of the average power meter and the reference pulse power meter the calibration curve of the latter is linked to absolute pulse power level. The dependence of the sensitivity of the cross-waveguide-type RS that serves as the reference pulse power meter during frequency response measurement is shown in Figure 7.

Making use of measurement techniques described in this section and 50 DC pulse supply for the RS feeding the output characteristics of the typical RS the electrophysical parameters of which are collected in Table 1 have been measured. Measured output signal dependence on pulse power is shown in Figure 8a by points. Two-term approximation (21) is represented by a solid line. For this particular case the values of coefficients $A = 25.43$ and $B = 36.30$ have been obtained. The resistance of the typical RS was roughly 16 Ω that corresponds to $\eta = 0.32$. As one can see from the figure, the approximation fits well experimental data. The dependence of the sensitivity on frequency for the typical X-band sensor measured in the linear region is shown Figure 8b. It is seen that sensitivity strongly depends on frequency with maximum to minimum ratio roughly 2.7. It might be concluded that reasons considered in

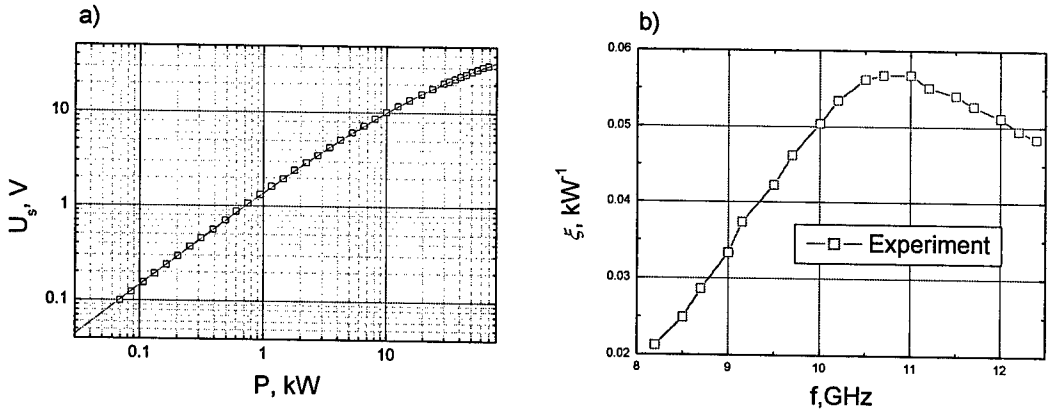

Figure 8. Measured output signal dependence on power at 9.3 GHz using 50 V DC pulse feeding of the RS (a) and the dependence of the sensitivity in the linear region on frequency (b) for typical X-band waveguide-diaphragm-type RS. Electrophysical parameters of the sensor are collected in Table 1.

subsection 2.2 that influences sensitivity dependence on frequency, namely: wave dispersion in the waveguide and electron heating inertia in a RF electric field, can not explain experimentally measured dependence. It seems that non-monotonous shape of $\zeta(f)$ is mainly caused by the dependence of the average electric field in the SE on frequency.

2.5 Conclusions

As follows from the presented results, the SE of the waveguide-type RS is sensitive to the average electric field strength in it. Even though electric field strength in the SE is equal to the electric field strength in the empty waveguide the sensitivity of the RS shall decrease by factor 1.44 in the waveguide's frequency band due to dispersion of wave in the waveguide. This decrease as well as electron heating inertia in microwave electric field can not explain experimentally observed non-monotonous sensitivity variation with frequency. Therefore, it can be concluded that observed sensitivity variation appears due to the dependence of the average electric field in the SE on frequency.

3. *Factors influencing the average electric field strength in the SE*

In the present section we discussed the influence of the electrophysical parameters of the waveguide-diaphragm-type RS on the value of the average electric field strength in the SE. Detailed consideration of this question can be found in the interim report [6]. Main principles employed for the RS frequency response engineering are described in this section.

3.1 Obstacle under the diaphragm

Considering electric field strength in a semiconducting obstacle under the diaphragm, it was shown [6] that at certain conditions some resonance might occur in such a structure. For the SE that influences considerably propagation properties under the diaphragm, odd quarter-wave resonance is likely prohibited since the SE is placed symmetrically in respect of edges of diaphragm, and distribution of fields should sustain same symmetry properties. Therefore, at a resonance conditions effective length of the transmission line under the diaphragm should become a whole number of half-wave only.

Our calculations have revealed [6] that for high specific resistance SE the increase of the average electric field in it has been observed when the even number of half-waves fits under the diaphragm. The example of one-wave resonance that is observed for $L_d = 25$ mm is shown in Figure 9. It is seen that at resonance conditions electric field amplitude exceeds E_0 up to three times. Maximum of the electric field at the edges of diaphragm is found. The increase of the cross-sectional area of the SE leads to the shift of the resonance frequency towards lower frequency as one can clearly see from the figure. This is not surprise, since increasing cross-sectional area of the obstacle the effective length of the transmission line under the diaphragm is increased.

When the specific resistance of the SE is reduced, the electric field strength in the SE decreases. It demonstrates calculation results shown in Figure 10. It is seen that for the smallest considered specific resistance the one-wave resonance does not manifest itself and monotonous decrease of the average electric field in the SE with increase of frequency is observed. Large reduction of $\langle E_m \rangle$ can be attributed to the fact that decrease of specific resistance enforces to form minimum of electric field in the SE instead of maximum that is characteristic to high specific resistance SE.

Investigating low specific resistance SE under the diaphragm, it was found that increase of the average electric field in the SE is observed when odd number of half-waves fits under the diaphragm. The example of three half-wave resonance that is observed for $L_d = 40$ mm is shown in Figure 11. It is seen that for ρ=1.25 Ωcm clear resonance peak is observed that

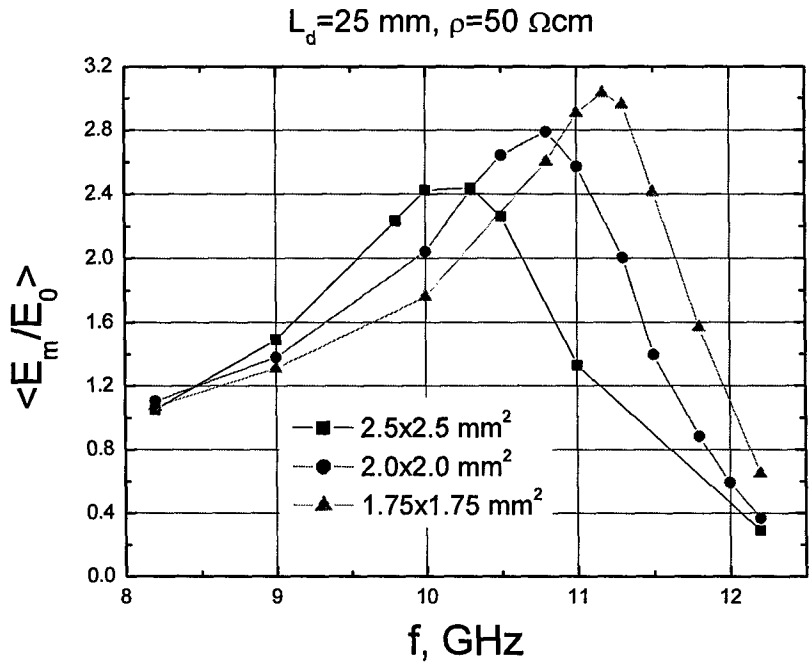

Figure 9. Calculated dependence of the average electric field strength in the SE normalized to electric field strength in the empty waveguide on frequency for different cross-sectional size of the SE: $h = 1$ mm, $L_d = 25$ mm, $\rho = 50$ Ωcm. Cross-sectional dimensions of the SE is indicated in the figure.

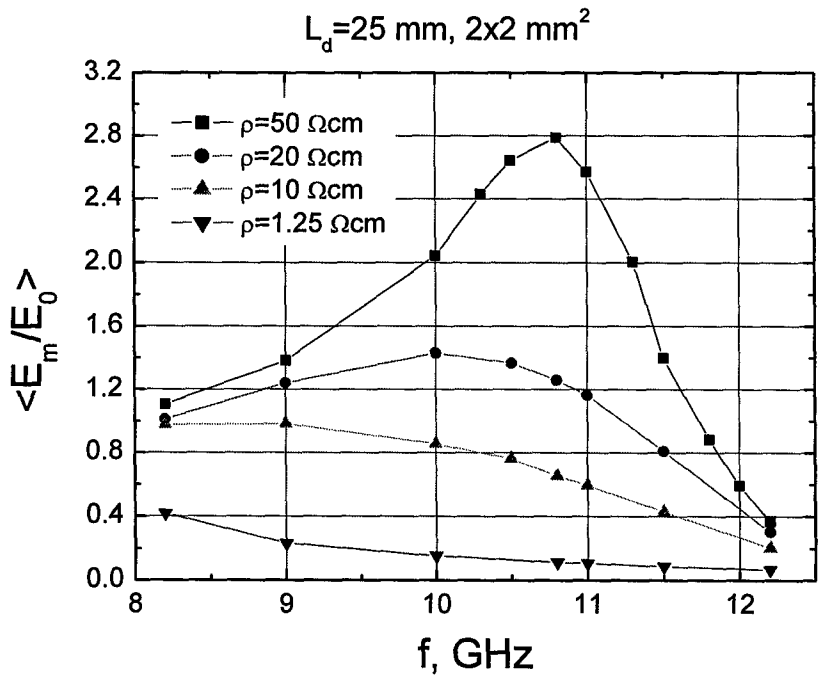

Figure 10. Calculated dependence of the average electric field strength in the SE normalized to electric field strength in the empty waveguide on frequency for different specific resistance of the SE: $L_d = 25$ mm, $h \times d \times l = 1 \times 2 \times 2$ mm^3. Specific resistance of the SE is indicated in the figure.

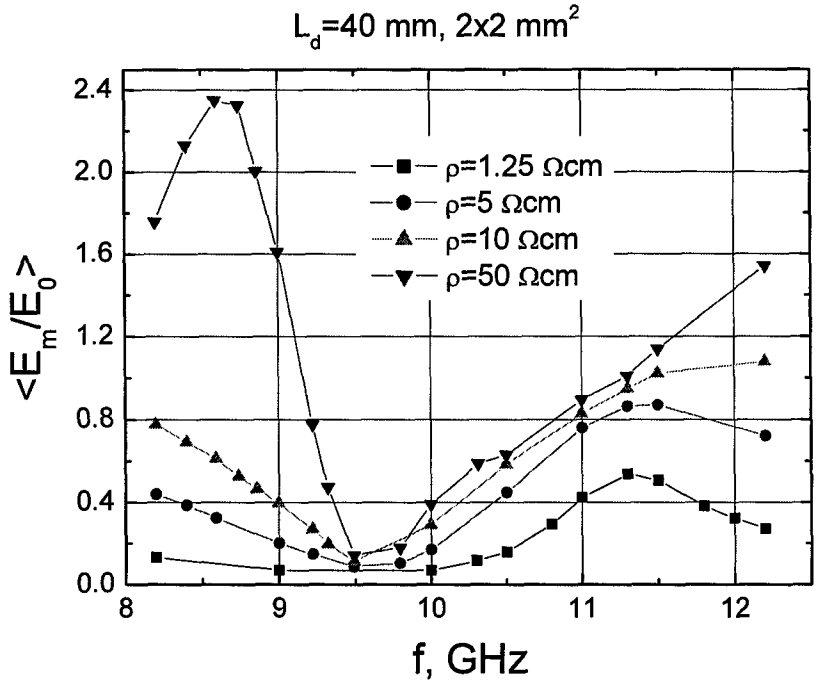

Figure 11. Calculated dependence of the average electric field strength in the SE normalized to electric field strength in the empty waveguide on frequency for different specific resistance of the SE: $L_d = 40$ mm, $h \times d \times l = 1 \times 2 \times 2$ mm^3. Specific resistance of the SE is indicated in the figure.

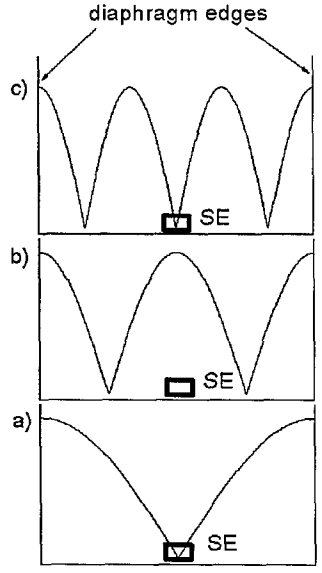

Figure 12. A sketch of the electric field distribution under the diaphragm at a resonance conditions: a) – half-wave, b) – one-wave, c) – three half-wave, a) and c) corresponds to the low and b) – high specific resistance SE.

reaches its maximum value at 11.3 GHz. Absolute value of the $\langle E_m \rangle$ is roughly four times lower in comparison with the amplitude of electric field in the case of high specific resistance SE at one-wave resonance considered earlier. It is seen, that the increase of ρ broadens the peak. It totally disappears for the highest specific resistance obstacle. For this case, $\langle E_m \rangle$ dependence on frequency is influenced by one-wave resonance in a low and two-wave resonance in high frequency regions only. The latter is outside waveguide's frequency band.

A sketch of electric field distribution under the diaphragm at one, two and three half-wave resonance conditions is shown in Figure 12. It is seen that the resonance takes place when electric field amplitude is maximal at the edges of diaphragm and whole number of half-wave fits under the diaphragm. Low specific resistance SE enforces the minimum of electric field in it while for high specific resistance – maximum of

electric field is characteristic.

Summarizing it should be pointed out, that electric field strength in the SE is influenced by resonance that occurs when a whole number of half-wave fits under the diaphragm. Both, the diaphragm length and cross-sectional size of the SE increase shits, in general, resonance maximum towards lower frequency. The resonance features manifests clearly itself either for low or high specific resistance SE. Therefore, the change of specific resistance of the SE leads to wider resonance peak or to its total disappearance. Taking into account the features of resonance mentioned above, the RS with desirable frequency response can be engineered.

3.2 Optimized sensor

Calculations that have been performed while optimizing the frequency response of the waveguide-diaphragm-type RS were described in detail in our previous report [6]. Therefore, we do not return to the details of the optimization procedure here.

Returning back to Table 1 one can found a set of electrophysical parameters that can be changed optimizing frequency response of the RS. Since the dimensions of waveguide window are fixed and we are considering square shape SE placed in the center of waveguide the number of parameters from 9 decreases to 4.

In the first step, the diaphragm length has been chosen. Next, by varying h in the range 0.5-2.0 mm, $d = l = 0.5$-3.0 mm and $\rho = 1.25$-50 Ωcm the optimal set of parameters has been selected. When choosing optimal set as a criterion maximum to minimum sensitivity ratio of the RS in waveguide's frequency band was used. It was also taken into account that the resistance of the SE should not exceed 50 Ω. Selected in such a way parameters of the waveguide-diaphragm-type RS with optimal frequency response are presented in Table 2.

Selection of specific resistance for the optimized sensor illustrates calculations results shown in Figure 13 where dependences of the average electric field on frequency for different

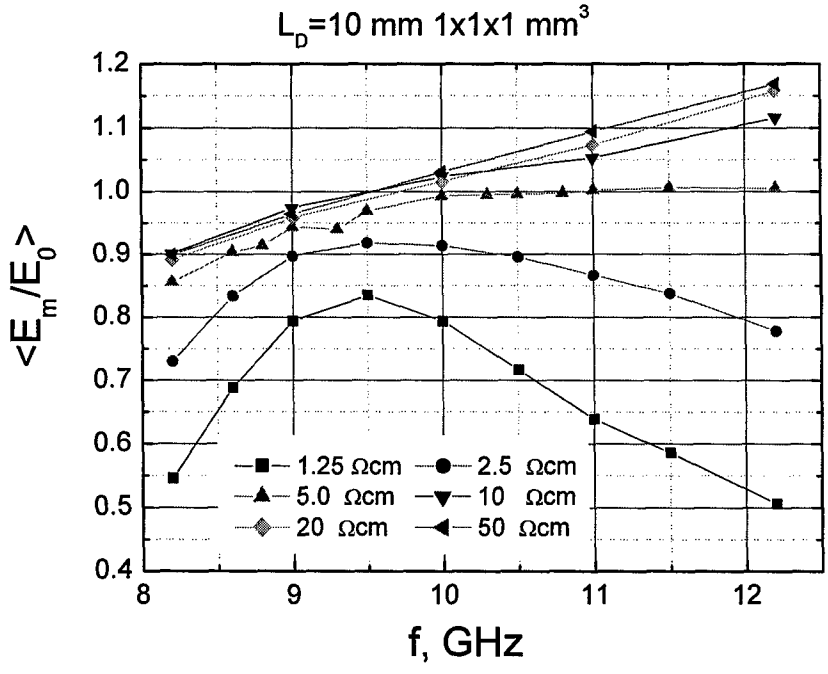

Figure 13. Calculated dependence of the average electric field strength in the SE normalized to electric field strength in the empty waveguide on frequency for different specific resistance of the SE: $L_d = 25$ mm, $h \times d \times l = 1 \times 2 \times 2$ mm^3. Specific resistance of the SE is indicated in the figure.

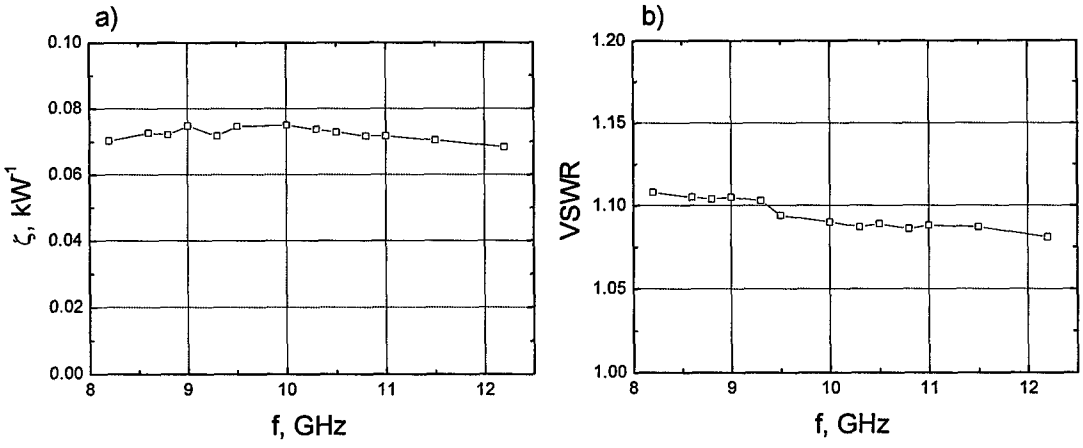

Figure 14. Calculated sensitivity (a) and voltage standing wave ratio (b) dependences on frequency for the optimized X-band waveguide-diaphragm-type RS. Parameters of the RS are collected in Table 2

Table 2. Electrophysical parameters of the waveguide-diaphragm-type RS with optimal frequency response.

a, mm	b, mm	h, mm	l, mm	d, mm	L_d, mm	ρ, Ω·cm	Δx, mm	Δz, mm
23	10	1.0	1.0	1.0	10.0	5.0	0.0	0.0

specific resistance are presented. The dimensions of the SE were held the same as for optimal RS. It is seen that for the lowest specific resistance of the SE considered, one half-wave resonance is observed. The increase of ρ broadens a peak. In a limit of high specific resistance, the monotonous increase of $\langle E_m \rangle$ influenced by one-wave resonance is observed. For $\rho = 5$ the increase of the average electric field with frequency nearly compensates the decrease of electric field due to wave dispersion in the waveguide and smooth frequency response was obtained.

Calculated sensitivity and voltage standing wave ratio (VSWR) dependences on frequency for optimized RS are shown in Figure 14. For this set of parameters minimum to maximum sensitivity ratio 1.09 was obtained. It is also seen that VSWR value is about 1.1 and slightly decreases with frequency.

3.3 Conclusions

Considering SE under thin metal diaphragm, it was found that the average electric field in it is strongly influenced by resonance occurring in such structure. For the SE made from low and high specific resistance material odd and even half-wave resonance appears. Resonance frequency depends on diaphragm length and cross sectional size of the SE. The increase of specific resistance in the case of odd resonance as well as the decrease of it in the case of even – leads to the broadening of resonance pike and to the total disappearance of it. Making use of this feature the RS with flat frequency response has been engineered by properly choosing the values of electrophysical parameters of the RS. For the optimal set of parameters, calculated maximum to minimum sensitivity ratio 1.09 in waveguide's frequency band was obtained.

4. Experimental investigation

Experimentally measured dependences of the sensitivity of the RS on frequency are presented in this section. Experimental results demonstrating the influence of the cross-sectional area of the SE and the diaphragm length on the RS sensitivity are described. Output signal dependence on pulse power for the optimized RS is also considered.

4.1 Frequency response

As it was already mentioned in section 3, electrophysical parameters of the waveguide-diaphragm-type RS with optimal frequency response for X-band have been determined [6]. They are collected in Table 2. Calculated maximum to minimum sensitivity ratio for this set of parameters was obtained 1.09. Therefore, our first objective was to manufacture the RS and measure their frequency response.

Five pieces of waveguide-diaphragm-type RS have been manufactured in accordance with electrophysical parameters collected in Table 2. Output signal dependences on frequency have been measured using technique described in section 2.4. From experimentally measured data, the values of sensitivity have been calculated making use of expression (22). They are shown in Figure 15 by points. Theoretically predicted sensitivity dependence on frequency is presented in the figure by solid line as well. To calculate the sensitivity of the RS expression (4) is employed. The amplitude of the average electric field strength $\langle E_m/E_0 \rangle$ in the SE was calculated using FDTD method. Detailed results of those calculations were presented in our previous report [6]. The influence of electron heating inertia on the value of β^* is taken into account using expression (5). The value of the warm electron coefficient in DC electric field $\beta = 6 \cdot 10^{-8}$ cm^2/V^2 for 5 Ωcm n-type Si [3] and $\tau_\varepsilon = 2.9 \cdot 10^{-12}$ s [7] was used in calculation.

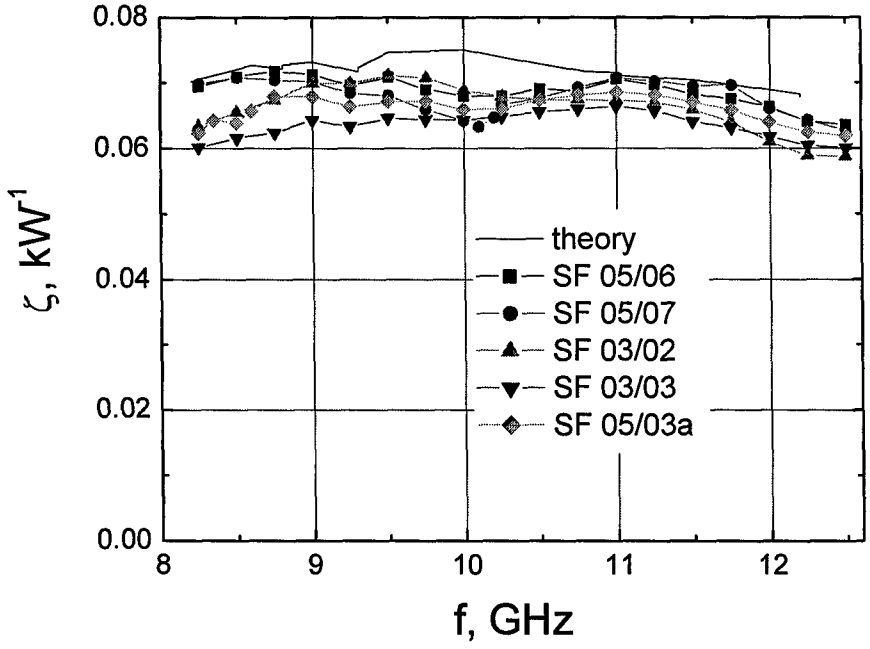

Figure 15. Measured dependence of the sensitivity in the linear region on frequency for the optimized X-band waveguide-diaphragm-type RS. Electrophysical parameters of the sensors are presented in Table 2. Points denote measurement results for different sensors, solid line represent calculated results.

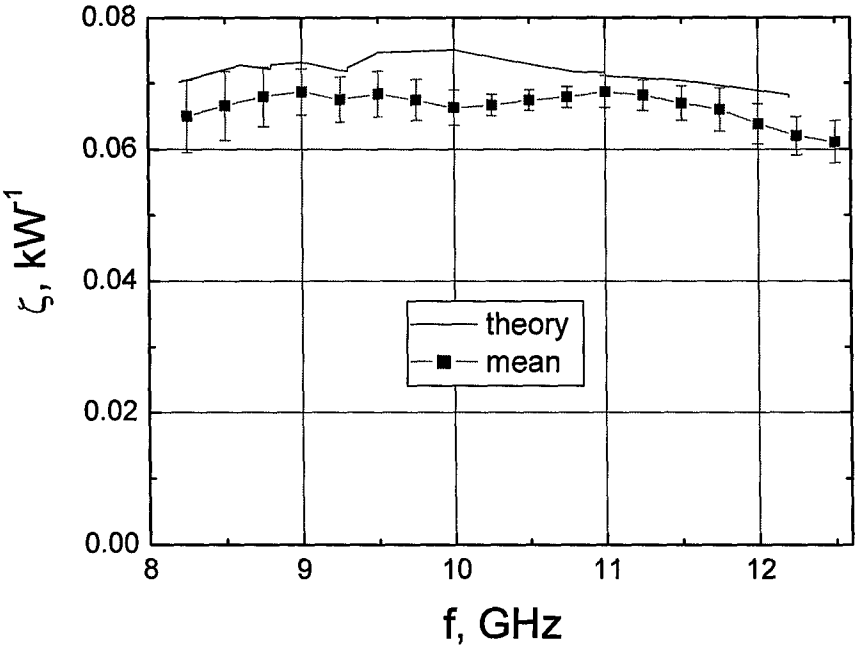

Figure 16. Dependence of the sensitivity in the linear region on frequency for the optimized X-band waveguide-diaphragm-type resistive sensor. Points denote averaged measurement results, error bars indicate standard deviation, and solid line represent calculated results.

As one can see from the figure, our experiments, in general, confirm theoretical predictions that the frequency response of the optimized waveguide-diaphragm-type RS should be smooth. It is seen that sufficiently low sensitivity variation with frequency is characteristic to the manufactured RS. The largest measured maximum to minimum sensitivity ratio for the particular RS does not exceed 1.2. Let us remind that as follows from calculations this ratio should be 1.09.

Having in mind possible scattering of electrophysical parameter of the manufactured RS, experimentally measured sensitivity values for different RS are sufficiently close to each other. The absolute value of measured sensitivity coincides well with calculated one. A small difference between the measured and calculated values can be attributed to size tolerances between the actual device and modeled prototype, to small mechanical displacement when installing the SE under the diaphragm, and to the measurement errors.

Averaged measurement results for different waveguide-diaphragm-type RS are shown in Figure 16. It is seen that the averaged dependence of the sensitivity on frequency is smooth: Maximum to minimum sensitivity ratio is 1.12. Comparing optimized sensor sensitivity with typical one that is shown in Figure 8b it is seen that the sensitivity of the optimized sensor increases particularly in a lower frequency region. Even maximal value of the sensitivity of the typical sensor is approximately 1.3 times smaller than the sensitivity of the optimized sensor. The sensitivity is about 3 times smaller in a lower frequency region. The point is that the average electric field strength in the SE of the optimized sensor is closer to the electric field strength in the center of the empty waveguide, i. e. $\langle E_m/E_0 \rangle \approx 1$, in a whole frequency range. Therefore, the perturbation that the RS introduces into regular waveguide is minimized.

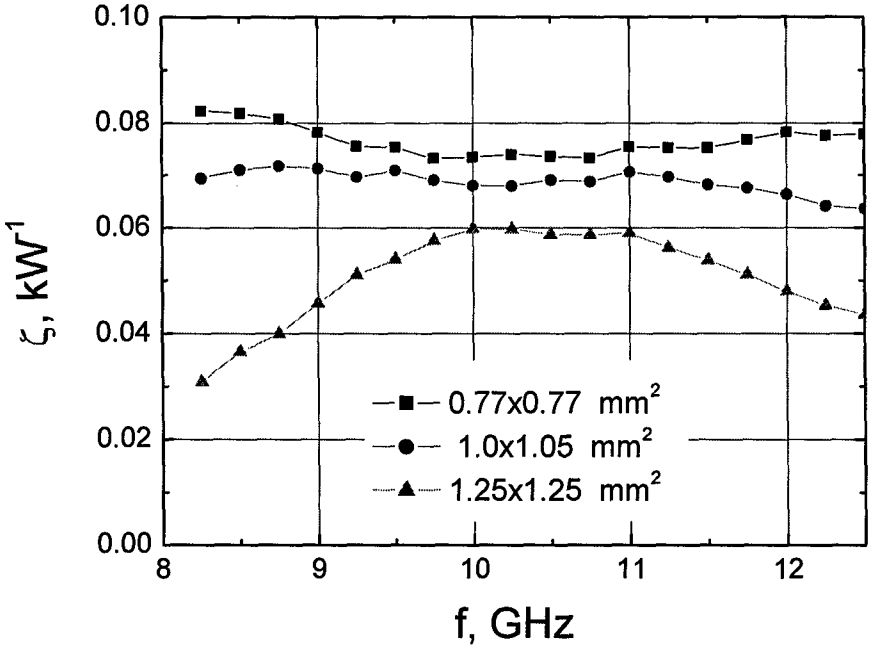

Figure 17. Measured dependence of the sensitivity in the linear region on frequency for the X-band waveguide-diaphragm-type resistive sensor for different cross-sectional area of the SE: $h = 1$ mm, $\rho = 5$ Ω·cm, $L_d = 10$ mm. Cross-sectional dimensions are indicated in the figure.

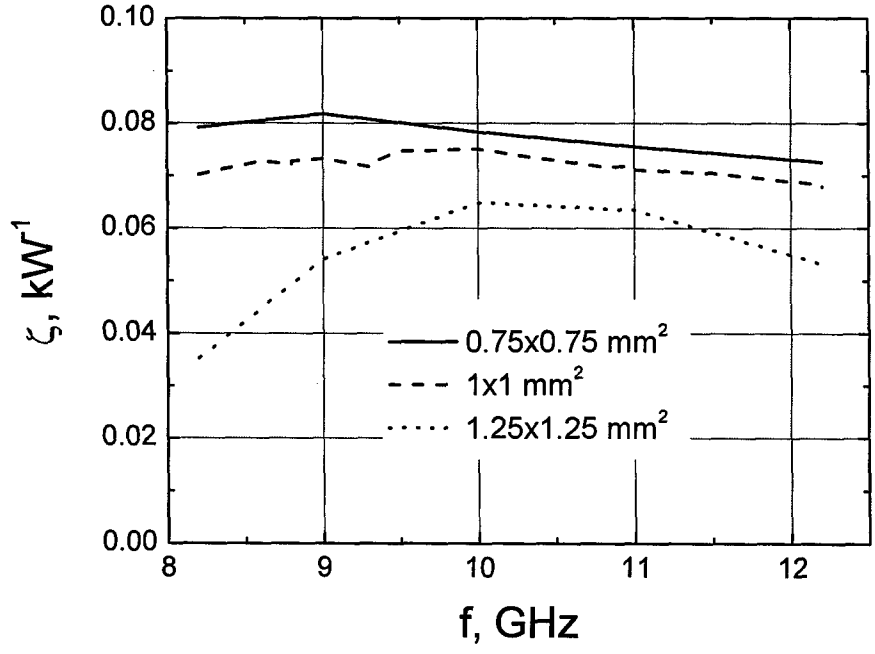

Figure 18. Calculated dependence of the sensitivity in the linear region on frequency for the X-band waveguide-diaphragm-type resistive sensor with different cross-sectional area of the SE: $h = 1.0$ mm, $\rho = 5$ Ω·cm, $L_d = 10$ mm. Cross-sectional dimensions are indicated in the figure.

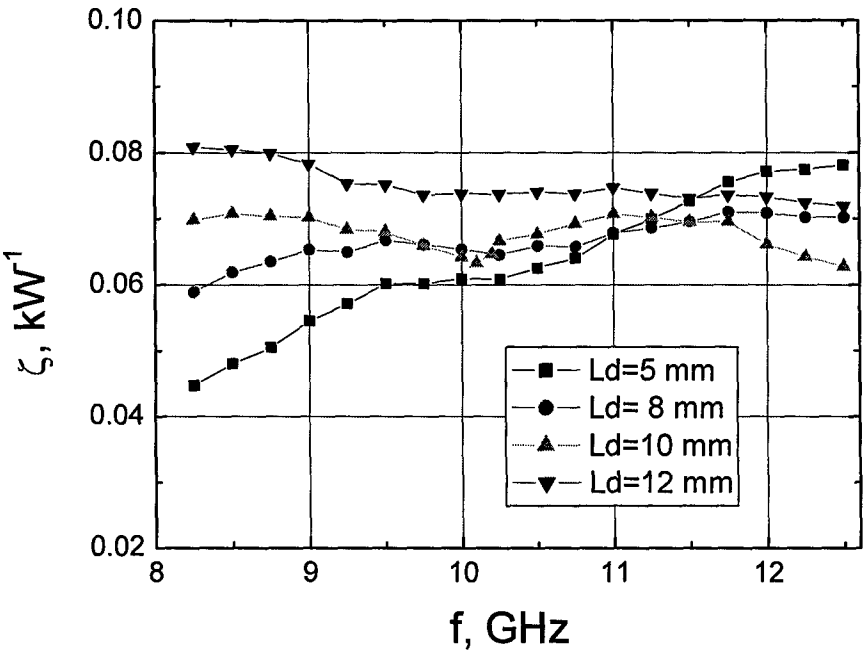

Figure 19. Measured dependence of the sensitivity in the linear region on frequency for the X-band waveguide-diaphragm-type resistive sensor for different length of the diaphragm: $h \times d \times l = 1.0 \times 1.0 \times 1.0$ mm^3, $\rho = 5$ Ω·cm, Diaphragm length is indicated in the figure.

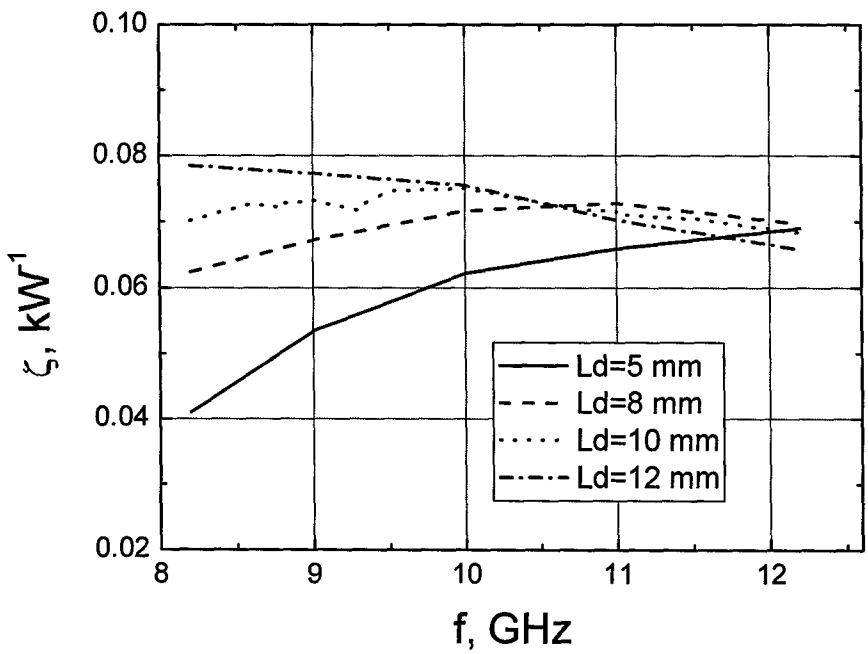

Figure 20. Calculated dependence of the sensitivity in the linear region on frequency for the X-band waveguide-diaphragm-type resistive sensor for different length of the diaphragm: $h \times d \times l = 1.0 \times 1.0 \times 1.0$ mm^3, $\rho = 5$ Ω·cm, Diaphragm length is indicated in the figure.

In the interim report [6] it was shown that small changes of the electrophysical parameters of the RS from their optimal value result in the increase of the sensitivity variation of the sensor in the frequency range under consideration. It lets believe that at least a local minimum of the sensitivity variation in a multidimensional space of the parameters has been found. We tried to prove this assumption experimentally.

Since the change of specific resistance of the SE, it is difficult to realize due to limited assortment of available n-Si ingots, two sets of experiments have been performed on the RS with slightly changed parameters only. The RS with the SE the cross-sectional dimensions of which is different from the optimal and the RS with changed length of the diaphragm have been investigated experimentally.

Experimentally measured sensitivity dependences on frequency for the RS with the different cross-sectional area of the SE are shown in Figure 17. The other electrophysical parameters of the RS were left optimal (Table 2). As it is seen from the figure the increase as well as the decrease of the cross-sectional area of the SE influences the frequency response curve of the RS. The resonance features of the electric field in the SE become more pronounced when the cross-sectional area of the SE is increased and the sensitivity dependence on frequency becomes non-monotonous. The decrease of the cross-sectional area of the SE has less influence on the frequency response. Calculated dependences of the RS sensitivity on frequency for different cross-sectional area of the SE are shown in Figure 18. It is seen that calculated dependences well coincide with measured ones.

Experimentally measured sensitivity dependences on frequency for the RS with the different diaphragm length are shown in Figure 19. As in the previous case the other electrophysical parameters of the RS were left optimal (Table 2). As one can see from the figure when the length of the diaphragm is increased the decrease of the sensitivity with frequency is observed and the opposite effect is observed when the length of diaphragm decreases. As it was already mentioned in section 3 the flat frequency response of the optimal RS is achieved due to the interplay of two phenomena that contrarily influenced the value of the average electric field in the SE. On the one hand, the average electric field strength in the SE decreases with frequency due to wave dispersion in the waveguide. On the other hand, the increase of the average electric field strength in the SE occurs when half-wave resonance conditions are fulfilled under the diaphragm. For the shortest diaphragm the resonance conditions are fulfilled in the vicinity of the highest frequency of waveguide's frequency band. Therefore, the increase of the average electric field in the SE with frequency exceeds the decrease due to wave dispersion and as a result the sensitivity of the RS increases with frequency. When the length of the diaphragm increases, the resonance shifts to the lower frequency region. It results in the decrease of the average electric field with frequency and the decrease of sensitivity with frequency is observed. Calculated dependences of the RS sensitivity on frequency for different length of the diaphragm are shown in Figure 20. It is seen that calculated dependences well coincide with measured ones.

4.2 Output signal

Output signal dependence on pulse power has been measured for the optimized RS as well. Measurement setup described in section 2.4 is used. Measurements were performed at a frequency 9.3 GHz using 50 V DC pulse supply for the RS feeding.

Typical measured output characteristic of the optimized waveguide-diaphragm-type RS is shown in Figure 21. Points represent experimental data; solid line shows two terms fitting of the experimental results making use of expression (21). It is seen that two terms approximation fits well experimental data in a whole pulse power range. As one can see from the figure more than twenty Volts signal is obtained at a maximum pulse power without any amplification.

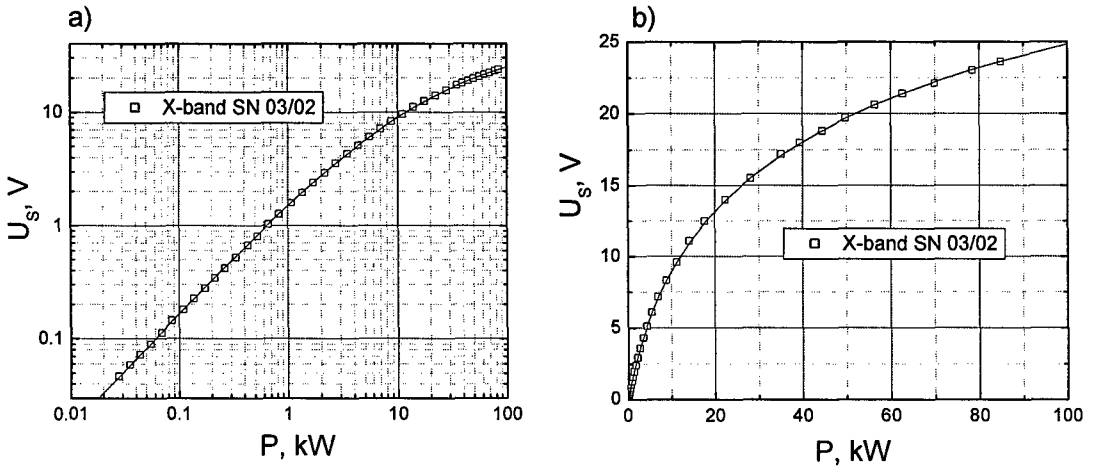

Figure 21. Output signal dependence on pulse power in waveguide of the optimized sensor SF 03/02 in logarithmical (a) and linear scale (b). Points denotes experimentally measured data, solid line shows two term approximation (21). Measurements have been performed at 9.3 GHz using 50 V DC pulse supply for sensor feeding.

Values of coefficients $A = 14.98$ and $B = 18.03$ have been obtained from the fitting. Comparing them with values obtained for a typical sensor ($A = 25.43$ and $B = 36.30$, Figure 8) it is seen that the sensitivity of the optimized RS increases about 1.6 times at 9.3 GHz. Comparing measured dependences in the linear region shown in Figure 8a and Figure 21a, one can find that roughly 0.15-0.16 V output signal will be obtained at a power 0.1 kW in both cases. Therefore, it might be concluded that the output signal in linear region is approximately the same for both sensors. The point is that the output signal of the RS depends not only on the sensitivity but also on the value of the ratio $\eta = R/R_a$ (21). This ratio increases from 0.32 for the typical sensor up to 1.0 for the optimized one reducing to zero the win in sensitivity. Sensitivity increase of the optimized sensor will manifest itself when measurements with the device having large input resistance will be performed ($\eta \to 0$).

The output characteristics of the other manufactured RS was similar to the results shown in Figure 21. The scattering of parameter A was in the interval of 10%. We also measured the VSWR for the manufactured RS. Measured maximal value was 1.16 and it slightly decreases with frequency as was predicted by our calculations (see Figure 14b). Discrepancy between calculated and measured values is sufficiently small and can be attributed to finite thickness of the metal diaphragm that is not accounted in the calculations.

4.3 Conclusions

A set of waveguide-diaphragm-type RS with improved frequency response has been manufactured and tested. Experimental results, in general, confirmed theoretical predictions that the frequency response of the waveguide-diaphragm-type RS can be significantly improved by properly selecting electrophysical parameters of it. Optimized RS is characterized by smooth dependence of the sensitivity on frequency. The largest experimentally measured maximum to minimum sensitivity ratio in waveguide's frequency band for particular RS was 1.2. That is sufficiently close to theoretically predicted value 1.09. Fairly good coincidence between values of the sensitivity of the RS calculated theoretically and measured experimentally was obtained. It was confirmed experimentally that small change of electrophysical parameters from their optimal values leads to the increase of the sensitivity variation in the frequency range under consideration.

5. Extension of dynamic range

As it follows from measurement results presented in a previous section the sensitivity of the optimized RS increases especially in a lower frequency region. As sensitivity increases the nonlinearity of the output signal dependence on power becomes more pronounced at higher power level and in this region measurement accuracy decreases. It was proposed to decrease the sensitivity of the RS by shifting the SE from the center of the waveguide towards its narrow wall [2]. This should allow extending the dynamic range of linear dependence of output signal to higher power level and, in general, designing the RS with desirable output characteristic. In the present section, we investigate the dependence of the RS sensitivity on the position of the SE shifted from the center of waveguide towards its narrow wall. The possibility to optimize the frequency response of such a sensor is also considered.

5.1 Shift of the sensing element

Frequency response of the RS with the SE shifted from waveguide's center has been investigated using FDTD method. The method and the model used in calculation are described in details in our previous report [6]. We only remind that calculated amplitude of electric field is normalized to the amplitude of electric field in the center of the empty waveguide of the ordinary wave H_{10} (3) and the shift of the SE is denoted as Δx.

At the beginning we investigated the dependence of the average electric field amplitude in the SE on frequency for the optimal RS, the SE of which is shifted towards narrow wall of the waveguide. Electrophysical parameters of the optimized RS are collected in Table 2. Normalized average electric field dependences on frequency for different Δx are shown in Figure 22. As one can see from the figure electric field strength in the SE decreases when it is shifted towards narrow wall of the waveguide. It is nothing surprising since moving from the center towards narrow wall the electric field component E_y in an ordinary H_{10} wave decreases. Unfortunately, the shape of the dependence $\langle E_m/E_0 \rangle(f)$ changes as well. It is seen that slight increase of electric field in the SE with frequency characteristic to the optimal RS changes to the decrease of $\langle E_m/E_0 \rangle$ in high frequency region when the SE is shifted from the center of the waveguide. Whereas the SE approaches to a narrow wall of waveguide the interaction of the SE with electromagnetic wave decreases and when it reaches the narrow wall ($\Delta x = 11$ mm), the average electric field strength in the SE becomes practically independent of frequency.

Calculated sensitivity dependences on frequency for the SE differently shifted from the center of waveguide are shown in Figure 23. It is seen that by changing Δx the sensitivity of the RS in a linear region can be changed in wide range. Comparing two limiting cases: the SE is placed in the center of waveguide ($\Delta x = 0$ mm) and the SE is pushed close to a narrow wall of waveguide ($\Delta x = 11$ mm), it is seen that sensitivity decreases roughly 150 times. It means that the output characteristic of the RS shown in Figure 21a can be shifted right in a power scale by 22 dB. Therefore, desirable output signal dependence on frequency can be engineered properly selecting the shift of the SE from the center of the waveguide. The modification of the output characteristic might be useful when measuring HPM pulse power close to waveguide breakdown. The example is shown in Figure 24 where the output characteristic of the optimized RS is extrapolated to higher power region making use of two term approximation (21). It is seen that measurement of HPM pulses in a range 100-200 kW with the optimized sensor should be less accurate due to strong nonlinearity of the output characteristic in this region. Better accuracy might be achieved by decreasing the sensitivity of the RS by 10 dB that can be easily realized in practice by shifting the SE from the center towards narrow wall roughly by 9 mm. The output characteristic for such RS is also presented in Figure 24.

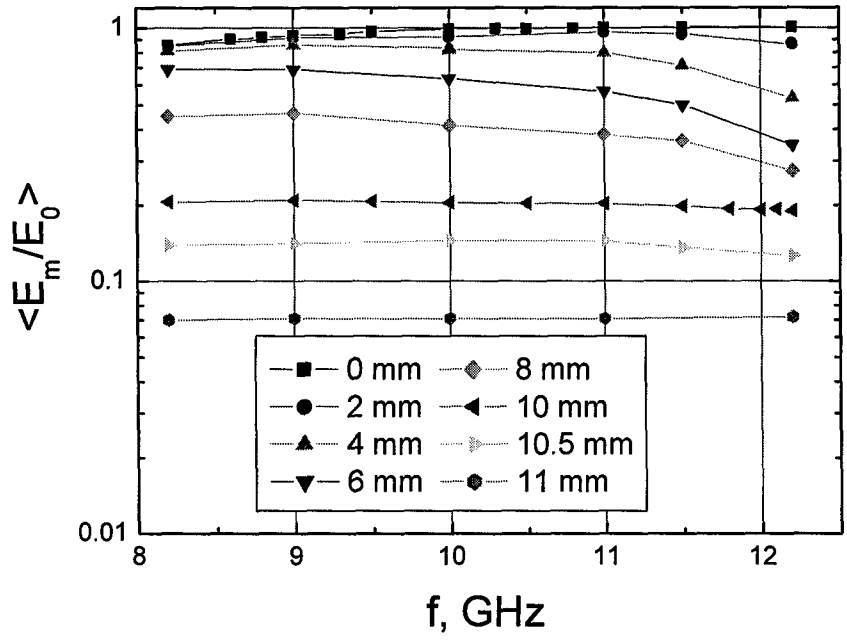

Figure 22. Calculated dependence of the average electric field in the SE on frequency differently shifted from the center towards narrow wall of the waveguide: $h \times d \times l = 1.0 \times 1.0 \times 1.0$ mm^3, $\rho = 5$ Ω·cm, $L_d = 10$ mm. Δx is indicated in figure.

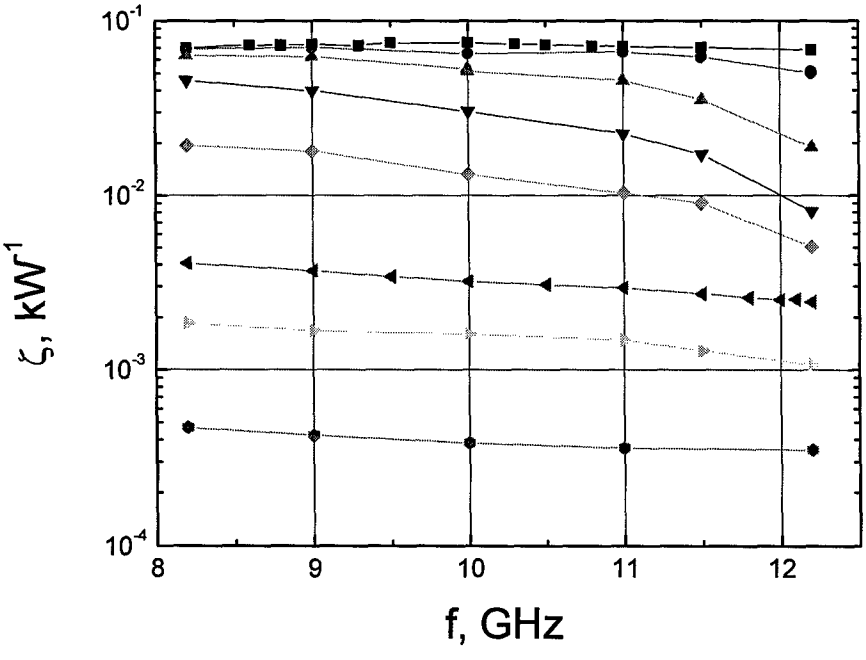

Figure 23. Calculated dependence of the sensitivity in the linear region on frequency for the X-band waveguide-diaphragm-type RS with the SE differently shifted from the center of the waveguide: $h \times d \times l = 1.0 \times 1.0 \times 1.0$ mm^3, $\rho = 5$ Ω·cm, $L_d = 10$ mm. Symbols indicating Δx value are the same as in Figure 22.

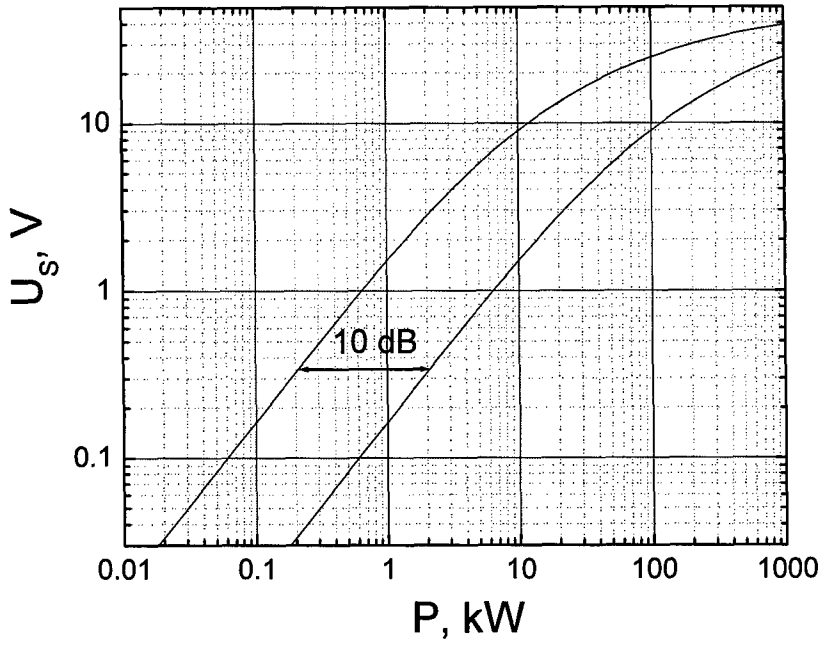

Figure 24. Output characteristic of the RS from Figure 21a extrapolated to higher power region using two term approximation (21) and for the RS with sensitivity decreased by 10 dB.

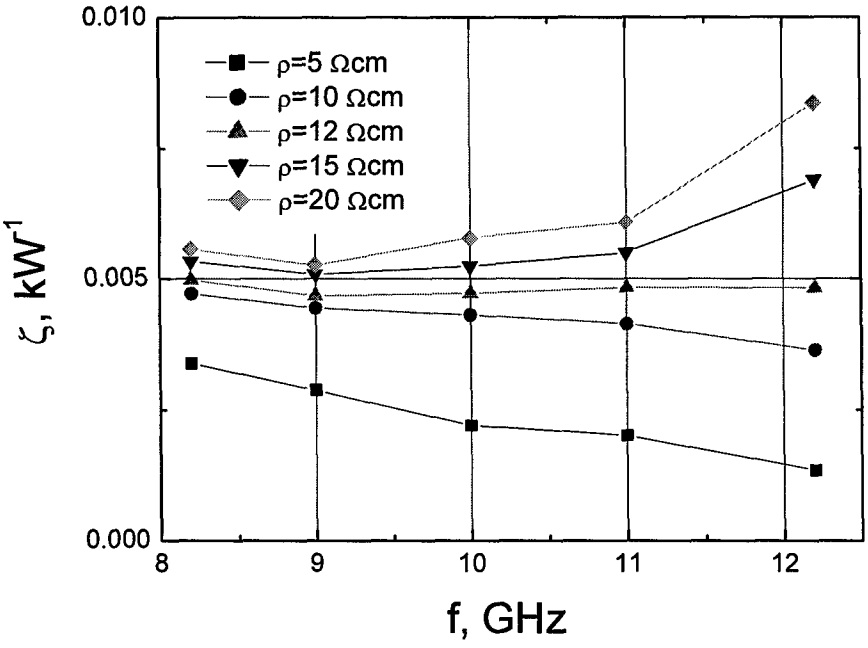

Figure 25. Calculated dependence of the sensitivity in the linear region on frequency for the X-band waveguide-diaphragm-type RS for different specific resistance SE shifted from the center of waveguide: $h \times d \times l = 1.0 \times 1.5 \times 1.5$ mm^3, $L_d = 10$ mm, $\Delta x = 10$ mm, specific resistance of the SE is indicated in figure.

5.2 Optimization of the characteristic of the RS with shifted SE

The frequency response of the RS with shifted SE can be optimized in a similar way as for the SE situated in the center of the waveguide. The example of such optimization is shown in Figure 25. The SE shifted at Δx = 10 mm, with dimensions $h \times d \times l$ = 1.0×1.5×1.5 mm^3 was investigated. The diaphragm length was L_d = 10 mm. It is seen that for SE made from 5 Ωcm specific resistance sensitivity decreases with frequency while the opposite dependence is characteristic to the higher specific resistance SE. Results of our investigation suggest that the average electric field strength in the SE is strongly influenced by one-wave resonance the frequency of which is somewhere in the higher frequency region outside waveguide's frequency band. As it was already shown in our previous report [6] the maximum of the average electric field is obtained within the high specific resistance SE at a one-wave resonance, which changes to minimum when the specific resistance of the SE decreases. Using this interplay the specific resistance can be found for which the sensitivity of the SE is a smooth function of frequency. As one can see from Figure 25 ρ =12 Ω·cm is the optimal specific resistance for this particular case providing flat frequency response of the RS.

5.3 Conclusions

The shift of the SE from the center towards the narrow wall of the waveguide provides the decrease of the sensitivity of the RS. Considering limiting cases for the optimized SE the sensitivity decrease by 22 dB was obtained. It was shown that the shift of the SE could be used for output characteristic engineering extending linear characteristic up to the higher power level. The frequency response of the RS with shifted SE was optimized making use of the fact that by decreasing specific resistance of the SE the maximum of the average electric field in the SE at one-wave resonance condition can be changed to minimum.

6. Conclusions

1. Factors influencing frequency response of the waveguide-diaphragm-type RS have been elucidated. It was shown that decrease of electric field in the waveguide with frequency due to dispersion of wave as well as electron heating inertia in microwave electric field can not explain non-monotonous sensitivity variation of the RS with frequency observed experimentally. Interaction of electromagnetic wave with the SE located under the thin metal diaphragm is responsible for the observed sensitivity variation.
2. Making use of FDTD method, the peculiarities of the interaction of the semiconductor bar inserted under thin metal diaphragm in the waveguide have been investigated. It was shown that the average electric field strength in the SE is influenced by resonance phenomena. Resonance occurs when the effective length of the diaphragm for wave propagating under it becomes a whole number of half-wave. Odd and even half-wave resonance can be distinguished. Odd resonance appears for low specific resistance, whereas even – for high specific resistance samples. Odd resonance disappears when the specific resistance of the SE increases whereas the decrease of specific resistance leads to disappearance of even resonance.
3. Varying electrophysical parameters of the waveguide-diaphragm-type RS (diaphragm length, dimensions and specific resistance of the sensor) and taking into account that the resistance of the RS should be less or equal 50 Ω the optimal set of parameters providing the smallest possible sensitivity variation in the waveguide's frequency band has been determined. They are: L_d = 10 mm, h = 1.0 mm, $d \times l$ = 1.0 mm^2, ρ = 5 Ω·cm. Calculated maximum to minimum sensitivity ratio for this set of parameters was obtained 1.09.

4. Theoretical predictions have been proved experimentally. The optimized RS is characterized by smooth dependence of sensitivity on frequency. The largest experimentally measured maximum to minimum sensitivity ratio in waveguide's frequency range for particular RS was 1.2. That is sufficiently close to theoretically predicted value 1.09. Fairly good coincidence between absolute values of the sensitivity of the RS calculated theoretically and measured experimentally was obtained. It was confirmed experimentally that small change of electrophysical parameters from their optimal values leads to the increase of the sensitivity variation in the frequency range under consideration.
5. A shift of the SE from the center of the waveguide is considered theoretically using FDTD method. It was shown that the shift of the SE might be useful for the engineering of more linear output characteristic of the RS in high power region. It was demonstrated that the frequency response of the RS with SE shifted from the center of the waveguide can be optimized as well.

7. References

[1] "Fundamentals of RF and Microwave Measurements," Application Note 64-1a, Hewlett Packard.

[2] M. Dagys, Ž. Kancleris, V. Orševkis, R. Simniškis, "Resistive Sensors for High Power Short Pulse Measurement in Waveguides", Electronics Letters, vol. 31, No. 16, p.1355-1357, 1995.

[3] M. Dagys, Ž. Kancleris, R. Simniškis, E. Schamiloglu, F.J. Agee, "Resistive Sensor: Device for High-Power Microwave Pulse Measurement", IEEE Antennas & Propagation Magazine, vol. 43, No 5, p. 64-79, 2001.

[4] M. Dagys, Ž. Kancleris, R. Simniškis, E. Schamiloglu, F.J. Agee, "X-Band Resistive Sensor for Short High-Power Microwave Measurement", 29th European Microwave Conference, Conference Proceedings, Munich, Germany, October 4-8, 1999, vol. 2, pp.65-68.

[5] S. Ramo, J.R. Whinnery, T. Duzer, Fields and Waves in Communication Electronics, John Wiley & Sons, New York, Chichester, Brisbane, Toronto, Singapore, 1984.

[6] "Improvement of Frequency Response of Waveguide-Type Resistive Sensors for High Power Microwave Pulse Measurement,"(Interim report), Microwave laboratory, Semiconductor Physics Institute, Vilnius, 2005.

[7] V. Dienys, Ž. Kancleris, and Z. Martūnas, "Electron Heating Inertia in Silicon at Room Temperature", Fiz. Tekh. Poluprovodn, vol. 13, No 9, 1706-1709, 1979 (in Russian).

8. Acknowledgement

The work is sponsored by the Air Force Office of Scientific Research, Air Force Material Command, USAF, under grant number FA8655-04-1-3047. The U.S. Government is authorized to reproduce and distribute reprints for Government purpose notwithstanding any copyright notation thereon.

The views and conclusions contained herein are those of the author and should not be interpreted as necessarily representing the official policies or endorsements, either expressed or implied, of the Air Force Office of Scientific Research or the U.S. Government.

The principal investigator Žilvinas Kancleris hereby declares that, to the best of his knowledge and belief, the technical data delivered herewith under Contract No. FA8655-04-1-3047 is complete, accurate and complies with all requirements of the contract. Disclosures of all subject inventions as defined in FAR 52.227-13 have been reported in accordance with this clause.